Clim. Past, 8, 609–623, 2012
www.clim-past.net/8/609/2012/
doi:10.5194/cp-8-609-2012

Climate of the Past

Centennial mineral dust variability in high-resolution ice core data from Dome C, Antarctica

F. Lambert[1,*], M. Bigler[2], J. P. Steffensen[2], M. Hutterli[3,], and H. Fischer[1]**

[1]Climate and Environmental Physics, Physics Institute, and Oeschger Centre for Climate Change Research, University of Bern, Sidlerstrasse 5, 3012 Bern, Switzerland
[2]Ice and Climate, Niels Bohr Institute, University of Copenhagen, Juliane Maries Vej 30, 2100 København Ø, Denmark
[3]British Antarctic Survey, High Cross, Madingley Road, Cambridge, CB3 0ET, UK
[*]now at: Korea Ocean Research and Development Institute, Ansan, Korea
[**]now at: Tofwerk AG, Uttigenstrasse 22, 3600 Thun, Switzerland

Correspondence to: F. Lambert (lambert@climate.unibe.ch), M. Bigler (bigler@climate.unibe.ch), J. P. Steffensen (jps@gfy.ku.dk), M. Hutterli (hutterli@bas.ac.uk), H. Fischer (hubertus.fischer@climate.unibe.ch)

Received: 2 March 2011 – Published in Clim. Past Discuss.: 4 April 2011
Revised: 21 February 2012 – Accepted: 11 March 2012 – Published: 22 March 2012

Abstract. Ice core data from Antarctica provide detailed insights into the characteristics of past climate, atmospheric circulation, as well as changes in the aerosol load of the atmosphere. We present high-resolution records of soluble calcium (Ca^{2+}), non-sea-salt soluble calcium ($nssCa^{2+}$), and particulate mineral dust aerosol from the East Antarctic Plateau at a depth resolution of 1 cm, spanning the past 800 000 years. Despite the fact that all three parameters are largely dust-derived, the ratio of $nssCa^{2+}$ to particulate dust is dependent on the particulate dust concentration itself. We used principal component analysis to extract the joint climatic signal and produce a common high-resolution record of dust flux. This new record is used to identify Antarctic warming events during the past eight glacial periods. The phasing of dust flux and CO_2 changes during glacial-interglacial transitions reveals that iron fertilization of the Southern Ocean during the past nine glacial terminations was not the dominant factor in the deglacial rise of CO_2 concentrations. Rapid changes in dust flux during glacial terminations and Antarctic warming events point to a rapid response of the southern westerly wind belt in the region of southern South American dust sources on changing climate conditions. The clear lead of these dust changes on temperature rise suggests that an atmospheric reorganization occurred in the Southern Hemisphere before the Southern Ocean warmed significantly.

1 Introduction

Atmospheric aerosol production, mobilization, long-range aeolian transport, and deposition respond to past climatic changes (Fischer et al., 2007b; Legrand and Mayewski, 1997; Mahowald et al., 2006a). In return, dust and other aerosols affect radiative forcing, thus climate, through absorption and scattering of incoming shortwave radiation (Mahowald et al., 2006b; Miller and Tegen, 1998; Tegen et al., 1996) and play a role as condensation nuclei (Sassen et al., 2003; Schwartz, 1996). The total atmospheric dust load as well as physical (e.g. size, shape) and mineralogical characteristics are important factors for the radiative budget of the atmosphere (Tegen, 2003), and for the micronutrient supply to terrestrial and marine ecosystems (Martin et al., 1991). The hypothesis that a reduced supply of iron to the Southern Ocean could be responsible for a substantial part of the 80–100 ppmv CO_2 increase from the Last Glacial Maximum (LGM) to the Holocene has been previously discussed (Martin et al., 1990; Watson et al., 2000). Estimates for the contribution of this iron fertilization to the total glacial/interglacial CO_2 difference range from $<20\,\%$ to $<40\,\%$ (Bopp, 2003; Martínez-Garcia et al., 2011; Ridgwell, 2003; Röthlisberger et al., 2004). It is commonly believed that a combination of iron fertilization, carbonate compensation feedback, and Southern Ocean ventilation

changes together with changes in ocean temperature drives the glacial-interglacial CO_2 changes (Bouttes et al., 2010; Fischer et al., 2007b; Köhler and Fischer, 2006; Sigman et al., 2010). Accordingly, documenting the centennial to millennial variability in dust input into the atmosphere and into the Southern Ocean is of great importance to constrain the impact of dust on the radiative budget and iron fertilization.

Insoluble mineral dust particles and soluble ionic aerosol constituents such as Ca^{2+} are transported through the atmosphere to remote polar areas, like the central East Antarctic plateau (Fischer et al., 2007b; Wolff et al., 2006). Many of these aerosol species (such as mineral dust) are non-volatile and irreversibly deposited onto the ice sheets (Legrand and Mayewski, 1997). Thus, they are regularly measured in polar ice cores and allow for conclusions concerning climatic processes in the aerosol source region and during transport of the past.

In the case of mineral dust, long-term changes have been documented during the last 800 000 years in low-resolution dust records from the Dome C ice core, Antarctica (Lambert et al., 2008), showing extraordinarily high dust fluxes during glacial conditions. Strontium and neodymium isotopic analyses identified southern South America ($>32°$ S) as the primary source for dust deposited onto the Antarctic ice sheet during recent climatic periods (Delmonte et al., 2004), with a stronger relative contribution from possibly Australian sources during recent interglacials (Delmonte et al., 2008; Revel-Rolland et al., 2006), and a possible additional source in the Puna-Altiplano in Argentina during glacials (Delmonte et al., 2010; Gaiero, 2007). The contribution of the exposed continental shelves during glacial times is unclear (Bigler et al., 2006; Maher et al., 2010); however, comparison of the temporal evolution in dust aerosol tracers and sea level during the last termination rules out that flooding of the previously exposed Argentinian continental shelf was the dominant factor for the dust changes during that time (Wolff et al., 2006).

Because calcium was more rapidly measurable at high-resolution in polar ice cores than particulate dust, it has routinely been used uncorrected (Ca^{2+}) or corrected for its sea salt contribution ($nssCa^{2+}$) as a proxy for mineral dust aerosol deposited in central Greenland (Fuhrer et al., 1999; Mayewski et al., 1994) or in central Antarctica (e.g. Fischer et al., 2007a; Röthlisberger et al., 2002). Particulate insoluble dust volume has been measured by the Coulter counter technique (e.g. Delmonte et al., 2002) at low-resolution. Laser absorption was additionally used for high-resolution particulate dust measurements (Ruth et al., 2002); however, size calibration of the absorption measurements is still a matter of discussion.

In this study we present for the first time the complete datasets of Ca^{2+}, $nssCa^{2+}$, and insoluble dust records (based on laser absorption measurements) from the Dome C ice core at 1 cm resolution spanning the entire past 800 000 years, obtained in the frame of the European Project for Ice Coring in Antarctica (EPICA). The calcium to particulate dust relationship is investigated during glacials and interglacials. Using principal component analysis (PCA), we produced a common dust flux signal that extracts the joint features of all our three dust proxy records. These new dust flux data are used to analyse millennial variability in the past eight glacial periods. We also investigate the possible causes and effects of dust variations and stepwise dust changes during glacial terminations.

2 Methods

The EPICA Dome C (EDC) ice core was drilled in East Antarctica (75°06′ S; 123°21′ E) and covers the last 800 000 years (Jouzel et al., 2007). From a depth of 24.2 m down to 3200 m, a Continuous Flow Analysis (CFA) system (Bigler et al., 2006, 2010; Röthlisberger et al., 2000) was applied to measure, among others, insoluble dust particles and soluble Ca^{2+} and Na^{+}. The data gathered with this method have a nominal depth resolution of $\sim$1 cm, taking dispersion in the CFA system into account, which corresponds to a formal sub-annual temporal resolution at the top and up to $\sim$25 years at the bottom of the ice core. Practically, surface snow mixing and dispersion in the ice result in a lower effective temporal resolution.

2.1 Calcium and non-sea-salt Calcium

For the ionic constituents the detection limit was about $0.2\,ng\,g^{-1}$ for Ca^{2+} and $3\,ng\,g^{-1}$ for Na^{+} (Bigler et al., 2006). The mean error for both Ca^{2+} and Na^{+} is estimated to be lower than $\pm 10\,\%$ (Bigler et al., 2006; Röthlisberger et al., 2000).

In contrast to particulate dust, Ca^{2+} has, apart from terrestrial, also marine sources (Bigler et al., 2006; Legrand and Mayewski, 1997). Although the marine aerosol ratio of Ca^{2+} to Na^{+} is well-known (Bowen, 1979), few studies have investigated the continental Ca^{2+} to Na^{+} ratio of terrestrial aerosols from specific regions (i.e. southern South America) (Bigler et al., 2006). However, these ratios are needed to calculate the exclusively terrestrial non-sea-salt calcium based on Ca^{2+} and Na^{+} measurements. The sea salt (ss) and non-sea-salt (nss) contribution to Na^{+} and Ca^{2+} can be calculated using the system of linear equations

$$\left[\mathrm{ssNa^{+}}\right] = \left(R_\mathrm{t} \cdot \left[\mathrm{Na^{+}}\right] - \left[\mathrm{Ca^{2+}}\right]\right) \cdot (R_\mathrm{t} - R_\mathrm{m})^{-1}$$

and

$$\left[\mathrm{nssCa^{2+}}\right] = R_\mathrm{t} \cdot \left(\left[\mathrm{Ca^{2+}}\right] - R_\mathrm{m} \cdot \left[\mathrm{Na^{+}}\right]\right) \cdot (R_\mathrm{t} - R_\mathrm{m})^{-1},$$

with R_t and R_m being the terrestrial and the marine Ca^{2+}/Na^{+} ratio, respectively (Bigler et al., 2006; Röthlisberger et al., 2002). Traditionally, the ratio R_m was assigned to the marine bulk sea water ratio of 0.038 and R_t to the average crustal value of 1.78 (Bowen, 1979). However,

sources other than sea spray, such as frost flowers, may have contributed significantly to the marine ion concentrations in central East Antarctica (Wolff et al., 2006). Based on these assumptions, an R_m value of 0.044 was proposed for Antarctic ice core data (Rankin et al., 2000). A study by Bigler et al. (2006) that estimated these ratios empirically using high-resolution CFA data from Dome C found $R_m = 0.043$ (±9 %) and $R_t = 1.06$ (±8 %) for the East Antarctic plateau. The lower R_t value, compared to Bowen (1979), most likely reflects the local crustal composition in southern South America. We used the marine and terrestrial Ca^{2+}/Na^+ ratios from (Bigler et al., 2006) in this study. Note that the difference in these parameters only marginally affects the calculation of $nssCa^{2+}$ in contrast to $ssNa^+$, which is not discussed here. Calcium and sodium data below the detection limit were discarded. Values below 0.1 ng g^{-1} (including all negative values) in the $nssCa^{2+}$ record were also discarded to avoid artifacts introduced by exceptionally high sodium concentrations, as the ratios R_t and R_m are, in principle, only valid on average and might not apply to single data points. Assuming an error of 10 % for Ca^{2+}, Na^+, R_m, and R_t, the uncertainty of the $nssCa^{2+}$ record amounts to ∼0.2 ng g^{-1} (30 %) during interglacials and ∼5.4 ng g^{-1} (10 %) during glacial maxima.

An additional analytical concern may be the amount of Ca^{2+} being leached from particulate dust after the ice sample has melted. This amount may be dependent on the acidity of the sample. Anomalously high Ca^{2+}/dust ratios were found, coinciding with volcanic eruptions (Ruth et al., 2002) in Greenland ice samples with very high Ca^{2+} concentrations. However, these occurrences are very localized and rare, and do not influence the long-term signal. In addition, the very good correspondence of Ca^{2+} concentrations measured by CFA and traditional ion chromatography (IC) (Ruth et al., 2008) excludes that a systematic offset is introduced during the CFA measurements. In the case of IC measurements, the melted sample gets in contact with the acidic IC eluent, which would lead to a higher solution of Ca^{2+} from particulate dust, if this were to be an important effect. Only for very low Ca^{2+} concentrations do the IC data divert to somewhat higher concentrations. However, this is due to the higher analytical blank of the discrete IC analysis. Accordingly, the CFA measurements can be regarded as reliable data of Ca^{2+} concentrations in ice core melted water. Note that this does not exclude a potential temporal variation in Ca^{2+} leaching of dust aerosol during atmospheric transport.

2.2 Insoluble dust

Insoluble dust concentration and size distribution below 769.5 m (from 44 to 800 kyr BP) were measured by laser-absorption particle sensors (Abakus from Klotz, Germany) (Ruth et al., 2003), in the following denoted as Bern dust data. The particle size detection limit of these laser particle devices (LPD) is approximately 1 µm of equivalent spherical particle diameter. The upper measuring limit was set to 17.2 µm. Within this size range the LPD counts the number of particles in 32 different size channels. The sum of all channels is then converted into an analogue voltage signal. In the Bern dust data this voltage signal was converted to number of particles per millilitre as described in Bigler (2004). The first 769.5 m were measured with a custom-made LPD from the University of Copenhagen featuring 4 channels only, and are referred to in the following as CPH dust data.

In principle, the particle size channels can be calibrated with spherical latex particles. In practice, however, this calibration proved insufficient, as mineral dust particles come in all shapes. Therefore, only the total dust particle number was used in this work, and an empirical calibration of dust mass fluxes was performed (see below) using low-resolution Coulter counter (CC) data (Lambert et al., 2008). Note that this calibration does not allow for a quantitative interpretation of dust size changes derived with the LPD. The error of the LPD dust particle number data is estimated to be <10 % (Ruth et al., 2002).

The lowest part of the ice core (below 3000 m) had many cracks and breaks, bearing the risk of contamination with drill fluid, whereas the rest of the core up to the end of the brittle zone (at ∼950 m) was essentially break free. Contamination with drill fluid compromises both LPD and CC measurements. They have caused either saturation of the LPD signal or were clearly recognizable based on unreasonably large size distribution data. In addition, the stratigraphy of the ice below 3190 m was disturbed and the climatic relevance of data collected in that part is strongly questioned (Jouzel et al., 2007). Therefore, only the data down to 3190 m depth are considered in this study.

2.3 Principal component analysis

The Ca^{2+} and $nssCa^{2+}$ concentrations, as well as the Bern and CPH dust particle number data are presented in Fig. 1. The light grey curve shows the 1 cm high-resolution data and the superimposed black curve shows discrete 55 cm median values. Note that the Bern and CPH particulate dust data have separate y-axes. All three species are considered proxies for atmospheric mineral dust concentrations, each with its own advantages and limits. Calcium has a low uncertainty, but is "contaminated" with $ssCa^{2+}$ during interglacials. The correction to $nssCa^{2+}$ removes the sea salt part at the cost of a lower accuracy due to the choice of R_t and R_m and a larger scatter at low concentrations. LPD particle number data have a low uncertainty for most of the record, but are not easily calibrated to mass concentration units. Principal component analysis (PCA) (e.g. Abdi and Williams, 2010) provides the means to extract the common climatic signal from all of these datasets. The low accumulation rate at Dome C and the log-normal distribution of dust proxy data make the logarithmic values of fluxes most representative for changes in atmospheric dust aerosol changes (Fischer et al., 2007b). Therefore, all datasets were multiplied with the accumulation rate

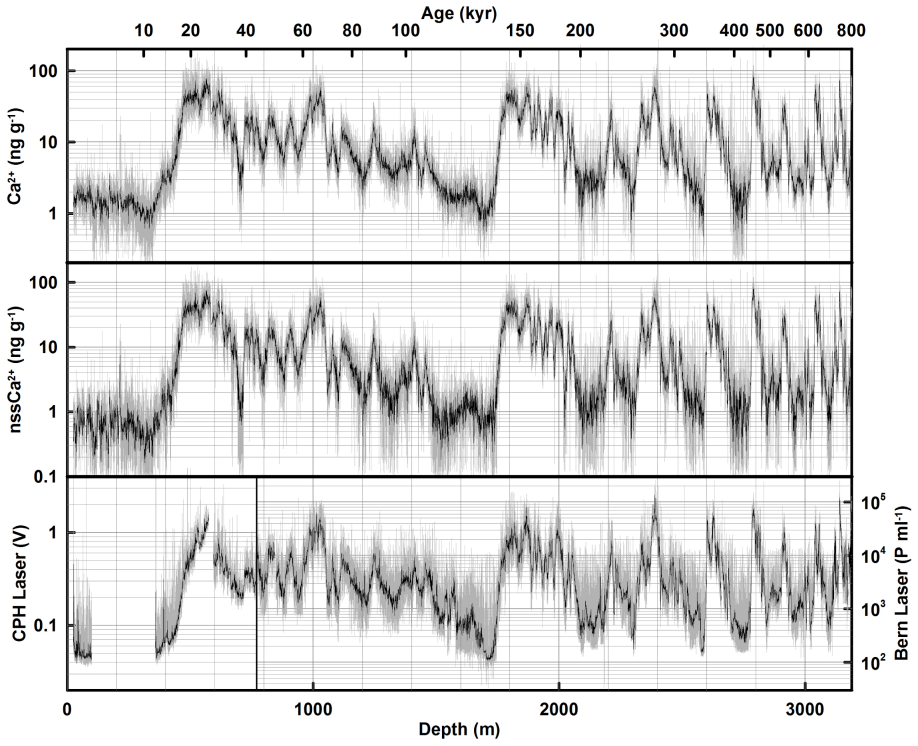

Fig. 1. Calcium, non-sea-salt calcium, and dust data at 1 cm resolution (grey), overlaid with 55 cm median values (black) from EPICA Dome C CFA on the depth scale. The EDC3 time scale in kyr is indicated on top. Dust was not measured between 100 and 358 m depth. Note that the CPH and Bern dust data have different y-axes.

and logarithmised prior to the PCA. Note that the accumulation rate is only available at 55 cm resolution (Jouzel et al., 2007) and that values in between were linearly interpolated.

In a first step, the CPH and Bern dust data had to be fused to one dataset. The CPH and Bern devices had different sensitivity, which resulted in different variability in the two data sections. To homogenize the two datasets, both were separated in a high-frequency and a low-frequency part by subtracting a smoothed record (we used a 1 kyr running mean with $\cos^2$ shaped weights) from the logarithmised flux data, essentially removing all glacial/interglacial variations from the high-frequency datasets. The high- and low-pass filtered CPH datasets were then standardized (i.e. centred and divided by the standard deviation) using their respective mean and standard deviation, and rescaled using the mean and standard deviation from the respective high- and low-pass filtered logarithmised Bern data in the section 120–165 kyr BP. This time section was chosen, because it is similar to the CPH data section in length and also encompasses both glacial and interglacial values. The resulting high and low frequency datasets were then added together and appended to the Bern data. We justify this procedure with the fact that both Ca^{2+} and $nssCa^{2+}$ show similar means and standard deviations (within 20 %) in high and low frequency bands in these two data sections. Nevertheless, one should keep this procedure in mind when analysing variability in the youngest part of the PCA-derived data.

In a second step we performed PCA using the three complete datasets (logarithmised Ca^{2+}, $nssCa^{2+}$, homogenized dust particle numbers). The first principal component (PC1) explains over 92 % of the variance in the records, and we interpret it as the mineral dust signal common to all three species. The rest of the variance stems from measurement uncertainty, sea salt influence, and noise. Gaps in the Ca^{2+}, $nssCa^{2+}$, and LPD datasets were linearly interpolated prior to performing the PCA. The linear interpolation is a good approximation of the average value, thus, the level of the PC1 data is not particularly affected. However, if there is a gap in one or two of the original records, the variance in PC1 will be decreased in that section (Fig. 2a). One has therefore to be careful when using the PC1 data to study dust flux variability in sections that feature large gaps in any of the original records.

2.4 Calibration

To calibrate the PC1 data to dust mass flux units, we used a two-sided regression analysis between PC1 and the logarithmised dust flux data from Coulter counter measurements. CC measurements were performed on discrete 7 cm long samples

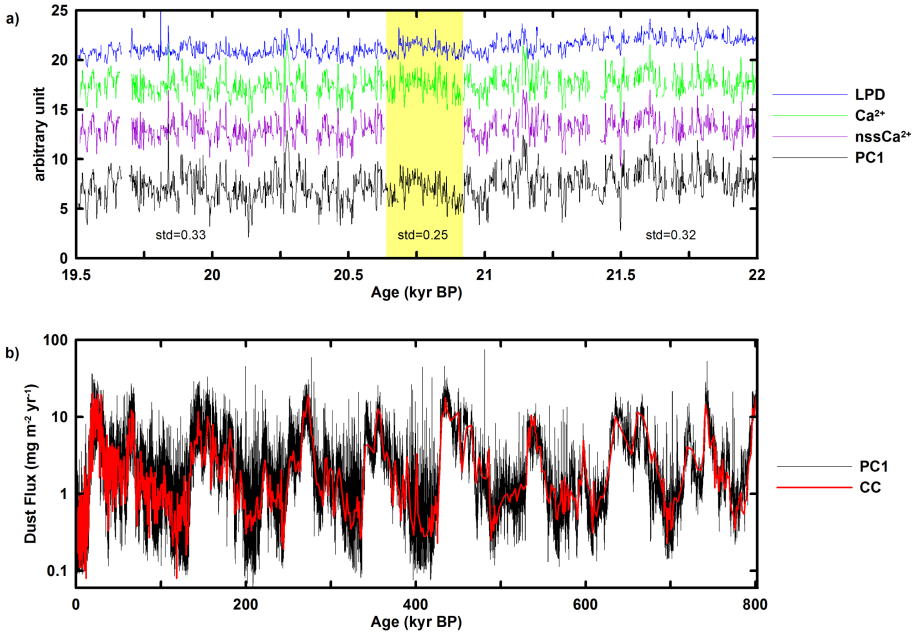

Fig. 2. **(a)** Example section featuring Ca^{2+}, $nssCa^{2+}$, and particulate dust data and the first principal component. Only where gaps are present in all three original datasets does the PC1 also feature a gap. The yellow band shows a section with reduced variability in PC1 due to a data gap in the $nssCa^{2+}$ record. **(b)** The first Principle Component (PC1) from the PCA (in black) has been calibrated with the Coulter counter dust flux data (in red) (Lambert et al., 2008).

at least every 6 m, but mostly every 55 cm over the whole EDC ice core. CC data and method are described in detail in Delmonte et al. (2002). The fit of the PC1 to the CC data was performed with averaged PC1 data of all 7 cm sections where CC measurements were available.

To estimate the error in the two-sided regression, we used a Monte Carlo approach, where we created 1000 ensembles of data points that scatter around the regression line with a distribution defined by the residuals of the original data points with the regression line. Note that the derived errors in the regression parameters reflect only the uncertainty in the regression itself due to the scatter of the entire dataset (as is the case for standard one-sided regression), but not the measurement error in each individual data point. This led to a Monte Carlo regression between logarithmic CC fluxes and PC1 according to

$$\log_{10}(\text{CC flux}) = (0.4925 \pm 0.0124) \cdot \text{PC1} + (0.1069 \pm 0.0065) \text{ with } r^2 = 0.83,\ n = 1028,$$

where CC flux is given in $\text{mg m}^{-2}\,\text{yr}^{-1}$. This translates to a relative calibration error of $<10\,\%$ for the dust flux values in the measured range between 0.1 and $50\,\text{mg m}^{-2}\,\text{yr}^{-1}$. The calibrated PC1 and the original CC data are plotted in Fig. 2b.

Note that with this calibration we avoided the issue of size calibration of the laser dust sensor. On the other hand, we cannot interpret differences in the evolution of soluble and particulate dust fluxes any more using our PC1-derived dust flux data. We therefore also calibrated the CPH and Bern LPD data individually, in a similar fashion with the CC concentrations (in ng g^{-1}), in order to compare particulate dust concentrations to calcium concentrations. The regression between logarithmic CC concentration and logarithmic Bern LPD data is

$$\log_{10}(\text{CC mass concentration}) = (0.9084 \pm 0.0309) \cdot \log_{10}(\text{Bern LPD data}) - (1.3276 \pm 0.1076) \text{ with } r^2 = 0.85,\ n = 519,$$

where CC mass concentration is given in ng g^{-1} and the Bern LPD data in particles ml^{-1}. The regression between the logarithmic CC concentration and rescaled logarithmic CPH LPD data is

$$\log_{10}(\text{CC mass concentration}) = (1.633 \pm 0.089) \cdot \log_{10}(\text{CPH LPD data}) + (3.136 \pm 0.128) \text{ with } r^2 = 0.80,\ n = 273,$$

where CC mass concentration is given in ng g^{-1} and the rescaled CPH LPD data in particles ml^{-1}. This translates to a calibration error in the range of 30–40 %, and 40–50 % for the entire range of dust concentrations (approximately 3–1500 ng g^{-1}) for the Bern and CPH dust data, respectively.

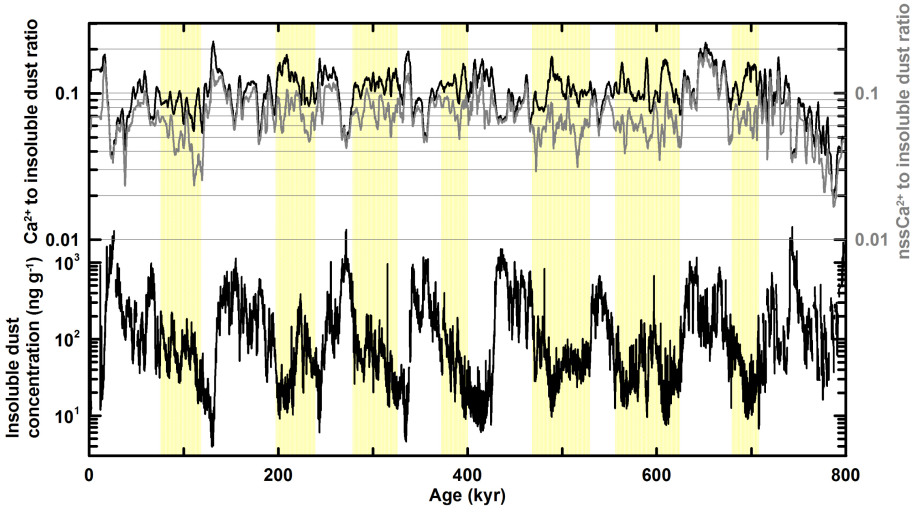

Fig. 3. Insoluble dust concentrations in ng g^{-1} with ratio of Ca^{2+} and dust (in black), and $nssCa^{2+}$ and dust (in grey) concentrations, using 100 yr median values on a logarithmic scale. Ratios have been smoothed by a 2500 year running average.

3 Results and discussion

3.1 Long-term trends in the insoluble dust to calcium ratio

Calcium and insoluble dust both follow the major climatic cycles with higher concentrations during cold times. We recorded typical interglacial concentration values of 1–2 ng g^{-1} for Ca^{2+}, 0.5–1 ng g^{-1} for $nssCa^{2+}$, and 200 particles ml^{-1} for insoluble dust (Fig. 1). During glacial maxima, average insoluble dust particle number concentrations increase by over two orders of magnitude, while Ca^{2+} and $nssCa^{2+}$ average mass concentrations increase by a factor of about 30 and 60, respectively. The particulate dust flux changes by a factor of 25–30.

Figure 3 (bottom panel) shows EDC insoluble dust mass concentrations during the past 800 kyr, with Ca^{2+} and $nssCa^{2+}$ to insoluble dust ratios in black and grey, respectively (top panel). The Ca^{2+} and $nssCa^{2+}$ to insoluble dust mass ratios fluctuate between about 0.03 and 0.2. Low and high ratios are generally related to glacial maxima and interglacials, respectively. The size of dust particles is unlikely to have played a role, as it stayed fairly constant over the record, with glacial-interglacial changes of only 5 % (Delmonte et al., 2004; Lambert et al., 2008). The higher interglacial values could have been related to a different mineral composition due to an additional dust input from Australian or even local Antarctic sources that had become insignificant relative to the total dust deposition during glacial times. Alternatively, interglacial Antarctic dust may have been subjected to a greater amount of Ca^{2+} leaching due to a change in weathering conditions on the way from its source, or was affected by changing ice alkalinity (Ruth et al., 2002). Interestingly, a clear change in dust composition has also been derived from He isotope measurements on mineral dust aerosol from the EPICA Dronning Maud Land ice core between the last glacial period and the Holocene (Winckler and Fischer, 2006).

Substantial discrepancies between the two ratios occur during periods with intermediate dust concentrations (yellow shaded areas in Fig. 3), which correspond to mild glacial conditions. The elevated Ca^{2+} to insoluble dust ratios, compared to $nssCa^{2+}$ to dust values during these time periods, indicate a higher $ssCa^{2+}$ content and therefore suggest a stronger transport of $ssCa^{2+}$ from coastal areas to the East Antarctic Plateau than during interglacial or full glacial conditions. This is also supported by the rather constantly high glacial sea salt aerosol fluxes ($ssNa^{+}$) despite $nssCa^{2+}$ fluxes changing by a factor of 5–10 from glacial inception to late glacial conditions (Fischer et al., 2007a).

It is interesting to note that the calcium to insoluble dust ratio changes its pattern before 700 000 yr BP. Taken at face value, these changes in the bottom part of the core point to a change in the crustal composition of dust transported to Antarctica during the climatic reorganization that happened during the mid-Pleistocene revolution. Note, however, that in this depth interval, single dust particles were agglomerated, possibly due to ice recrystallization and shear deformation processes (Lambert et al., 2008). This could potentially affect the leaching of Ca^{2+} from these aggregates.

3.2 High-resolution dust flux changes

In Fig. 2b we show the calibrated PC1 dust flux dataset. It is shown in black with the Coulter counter dust flux data (Lambert et al., 2008) overlaid in red. As the common signal found in the high-resolution particulate dust, Ca^{2+}, and $nssCa^{2+}$ data, PC1 can be interpreted as the best representation of

high-resolution atmospheric mineral dust variability. Being empirically calibrated against dust mass fluxes from CC measurements, the amplitude of the changes reflects that of insoluble particulate dust fluxes. The dataset ranges from 400 to 801 000 yr BP with a resolution of 1 cm. This corresponds to a formal three-month resolution at the top to ∼25 years at the bottom of the core. Average dust flux values vary between 0.2–0.6 mg m^{-2} yr^{-1} and 10–30 mg m^{-2} yr^{-1} during interglacials and glacials, respectively.

3.2.1 Dust imprint during Antarctic warming events

Antarctic warming events like the ones reported in stable water isotopes as intermittent Antarctic Isotope Maxima (AIM) during the last glacial period (Blunier and Brook, 2001; EPICA community members, 2006) are interpreted as periods of accumulating heat in the Southern Atlantic Ocean, most likely related to a weakening of the Atlantic Meridional Overturning Circulation (AMOC) during stadial conditions in the North Atlantic, and a rapid restart of the AMOC at the onset of Dansgaard-Oeschger (DO) events (Stocker and Johnsen, 2003). A recent study suggested that, during the last glacial period, every DO event had a corresponding AIM (EPICA community members, 2006). Similar millennial features have also been recorded in previous glacial periods in Antarctic water isotope records and CH_4 concentrations derived from the Dome C ice core, suggesting that millennial scale variability was a persistent feature during glacial periods (Jouzel et al., 2007; Loulergue et al., 2008; Martrat et al., 2007).

Antarctic dust flux and temperature variations are very well correlated during glacial times (Lambert et al., 2008). This tight link between dust and climate allows us to use our dust flux record as a first order indicator of Southern Ocean millennial climate variability. In Fig. 4 we present a 25-year average of the dust flux during glacial periods in black, underlain with the EDC isotope temperature (Jouzel et al., 2007) in grey. Note that the lower resolution of the EDC δD data, as well as the smoothing of the isotope record by diffusion in the ice, limit the recognition of warming events in the deeper core. Our high-resolution dust mass flux record is not subject to these limitations. Even before 740 kyr BP, where aggregation of dust particles in the ice occurred, we see no major effect of this process on the dust mass flux reconstruction. A comparison of the EDC δD data with our dust flux record during the last glacial period shows that all the AIMs can also be seen in the dust record. Using our dust flux data, we can identify the potential Antarctic warming events during every glacial period back to Marine Isotopic Stage (MIS) 18 and name them according to the MIS they occurred in. The identification was performed by subtracting a 3 kyr running median from a 1 kyr running mean with $\cos^2$-shaped weights using centred logarithmic dust flux values. This essentially represents a band-pass filter for variations in the dust flux of the typical length of Antarctic warming events. All negative sections in the difference record that were longer than 700 years and had an area >1.5 were defined as warming events. The four parameters of the detection algorithm (length of the window and percentile value of the running percentile (we also tried other values other than the median), length and area of the section in the difference record) were calibrated for the last glacial period so as to detect all and only the AIMs.

The detection method appears to produce very good results. All major and almost all minor events in the dust record are detected. There are two possible exceptions at 261 and 366 kyr BP where potential events were missed by the algorithm. There are also some events (6.2, 6.12, 12.3, 16.4, 18.1) that appear dubious to the eye and may be false positives. We have compared our warming events with the predicted occurrence of DO events based on EDC isotopic data (Barker et al., 2011). The predicted DO events have been marked with a triangle in Fig. 4. Dating back to 310 kyr BP the predicted DO events coincide very well with the imprint of Antarctic warming events in the dust data. However, before 340 kyr BP the time resolution of the isotope data drops quickly to more than 300 years per 55 cm, and some smaller potential events are only found in our data.

In summary, millennial variability in the Southern Hemisphere was a persistent feature during all glacial periods in the past 800 kyr. The centennial to millennial climate variability in the Southern Ocean region prior to 340 kyr BP was somewhat higher than derived by Barker et al. (2011), and more DO events are likely to have taken place at that time in the North Atlantic region. The rate of occurrence of Antarctic warming events is fairly constant around 2–3 events per 10 kyr. We confirm prior findings with a tendency towards maximal variability during intermediate climatic states and low variability during climatic extremes (Wolff et al., 2009). However, small events did happen regularly also during glacial maxima just prior to each termination, which suggests that the bipolar seasaw was not completely inactive during those times.

3.2.2 Dust changes during transitions

The unprecedented resolution of our dataset allows also for a precise analysis of the timing of dust changes and of leads and lags with other parameters during climate transitions. Figure 5 highlights the behaviour of mineral dust during the last nine glacial terminations. Dust flux is shown in brown at a 25 year resolution during all transitions, with the 1 cm data in grey in the background. We compared our dust record to the EDC isotope temperature record in black (Jouzel et al., 2007) and the EDC and Vostok CO_2 stack in red (Lüthi et al., 2008).

Against common practice, dust has been plotted on a linear scale to emphasize at which point in time the flux had dropped to levels close to the interglacial minima, where subsequent changes should not have significantly affected iron

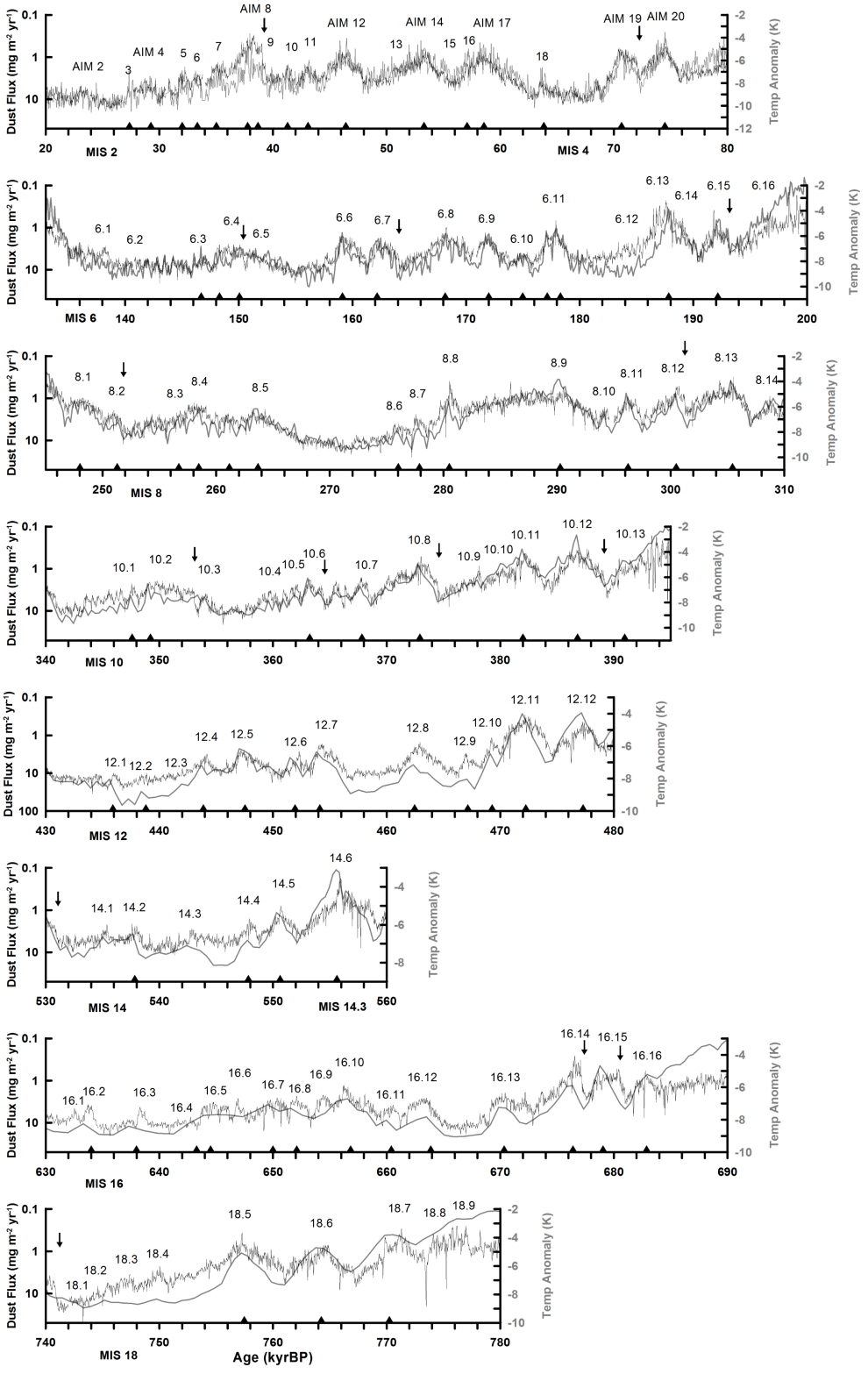

Fig. 4. 25 year mean dust flux data in black underlain with the EDC temperature data at original 55 cm depth resolution (Jouzel et al., 2007) back to 800 kyr BP. Antarctic Isotopic Maxima (AIM) during the last glacial are marked as identified in EPICA comm. Members(2006). Previous warming/low dust events as detected in our high-resolution dust record have been consecutively numbered according to their Marine Isotope Stage. Vertical arrows mark the rapid dust flux jumps. The triangles mark the predicted occurrence of DO events based on the EDC δD data (Barker et al., 2011).

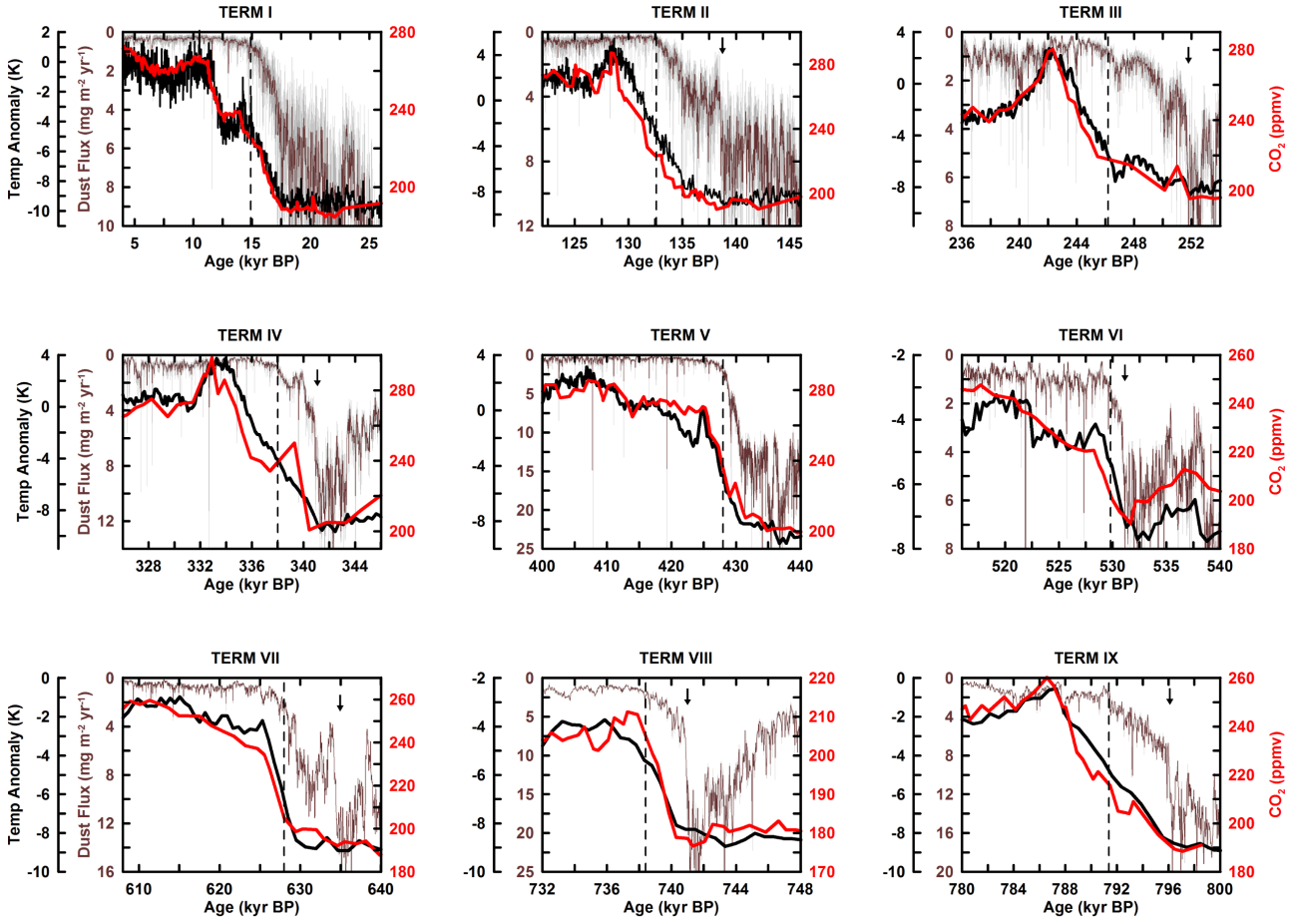

Fig. 5. Evolution of dust flux (on an inverted axis at 1 cm resolution in grey overlaid with a 25 yr mean in brown), EDC temperature (Jouzel et al., 2007 in black) and CO_2 concentrations (Lüthi et al., 2008 in red) during the past nine glacial terminations. The dashed line marks the time when dust flux reaches interglacial conditions. Vertical arrows mark the rapid dust jumps.

fertilization in the Southern Ocean. This time value has been marked with a dashed vertical line. Although the precise moment when dust reaches interglacial levels can be argued, it is clear that in all glacial terminations this moment was reached in dust flux well before temperature and CO_2 reached interglacial levels. This dust lead on temperature and CO_2 maxima is surprisingly consistent around 4 kyr and much larger than the uncertainty in the gas age-ice age difference. It is also easy to see that even when CO_2 and dust flux start changing at approximately the same time, CO_2 levels continue rising steadily long after dust has reached interglacial values. In addition, during every termination, CO_2 levels were still rather low (200–240 ppmv) by the time the dust-borne iron supply to the Southern Ocean had been reduced to interglacial levels. This shows that the continuing increase in CO_2 after the dust drop cannot be related to a reduction in iron fertilization. Termination I and V show the largest CO_2 concentration rise of ∼30 ppmv at the time dust reaches interglacial levels, which corresponds to about 30 % of the total glacial-interglacial change. Other terminations show much smaller CO_2 increases concurrent with the dust decrease. Previous studies have postulated a link between the aeolian iron influx into the Southern Ocean and CO_2 levels through the biological productivity of micronutrient limited regions (Maher et al., 2010; Martin et al., 1990). Martínez-Garcia et al. (2009) inferred an exponential relationship between export productivity and atmospheric CO_2 levels, with the highest sensitivity occurring during glacial maxima. Such an exponential relationship is reminiscent of the connection between atmospheric dust and climate and one could imagine a direct link between dust-borne micronutrients and biological productivity. However, Fig. 5 shows that although dust and CO_2 changes were simultaneous during the last glacial-interglacial transition, this was not necessarily the case during earlier terminations. Many terminations show large reductions in dust influx (see arrows in Fig. 5) that have no counterpart in the CO_2 record. We conclude that during glacial maximum conditions, the biological productivity was not necessarily limited by aeolian-borne micronutrients. We can therefore confirm the conclusion of previous studies that

iron fertilization of the Southern Ocean is unlikely to have played a dominant role in CO_2 concentration changes during the last termination (Bopp, 2003; Fischer et al., 2010; Ridgwell, 2003; Röthlisberger et al., 2004), and extend it to glacial terminations in general.

A special feature of the dust flux is that in most cases it did not gradually change from glacial to interglacial levels as temperature and CO_2 did. During most terminations the dust flux data show one or more sudden, very fast drops that happen within a few centuries (indicated by vertical arrows in Fig. 5). These sudden jumps occur during all transitions, although they are not as pronounced during terminations I and V, when the dust flux falls more gradually towards interglacial levels. Clearly, the amplitude of these jumps is not as marked when using logarithmic dust flux data (as justified by the approximately log-normal distribution of dust fluxes for constant climate conditions), but the jumps are still prominent with respect to the rapidity of the step-like changes.

A recently proposed reason for the early drop in dust export from Patagonia during the last termination is that glaciers retreated into proglacial lakes (Sugden et al., 2009). Before 20 kyr BP, glaciers discharged onto outwash plains, and dust mobilization was consequently high. In contrast, it is suggested that glaciers terminated in glacial lakes after 18 kyr BP trapping dust provided by glacier outwash. We cannot rule out that the abrupt dust drops observed during the transitions may have been caused by this process. However, it is unlikely that all proglacial lakes were repeatedly formed within a few centuries of each other.

Another more likely reason for the fast decline of dust flux during glacial terminations is a sudden change in atmospheric circulation and the hydrological cycle over the dust source regions. Increased moisture in previously arid regions may have allowed vegetation to grow quickly, which would have significantly hindered the dust mobilization into the atmosphere. In addition, an enhanced hydrological cycle would have reduced the lifetime of airborne dust particles during transport by increasing washout, thus, reducing the amount of dust exported to far away regions (Lambert et al., 2008).

One possible reason for such a sudden change in the hydrological cycle of southern South America could be a latitudinal shift or change in extension of the westerly wind belt connected to the deep pressure trough and the region of intense cyclonic activity in the Southern Ocean. Dust mobilization in southern South America today is mainly occurring during summer, when precipitation is low and individual high wind events can pick up dust aerosol. High wind speeds are connected to cyclones passing the Drake Passage and thus episodic in character (Lässig et al., 1999). Further to the north, zonal wind conditions crossing the Andes lead to föhn conditions (Zonda wind) lee sides of the mountains (Lässig et al., 1999), connected to high wind speed and potentially dust uptake. It has been suggested that the position of the Westerlies over South America varies according to sea surface temperature (Lamy et al., 2010). During cold conditions, the region of high westerly wind may expand northward (as is the case for recent winter conditions), making cyclonic influence in southern South America less episodic and zonal winds more steady. In addition, the dryer conditions during glacial times connected to a constant replenishment of fluvial dust sources by enhanced glacial outwash, lead to a combination of high dust supply and strong wind uptake at that time. As temperature rises, the wind belt contracts while the wind intensity in the core may increase (as observed in summertime today). Also, precipitation in Patagonia may increase again, suppressing dust mobilization and prompting vegetation to grow on previously dusty soil.

As illustrated in Fig. 5, the rapid stepwise dust increases occurred very early during the deglaciation, i.e. when temperatures were still low and glacier extent in Patagonia still close to its maximum. Therefore, a thermodynamic effect on precipitation rate and washout of aeolian dust at that time is still expected to be small. However, at this time Na^+ concentrations in the ice core also started to decline, pointing to a reduction in sea ice and/or storminess in the Southern Ocean (Bigler et al., 2010; Wolff et al., 2006). Accordingly, we conclude that the strong stepwise change in dust mobilization and transport to the Antarctic ice sheet observed in our record at the beginning of the terminations is more likely connected to a rapid atmospheric reorganization at that time. This is also supported by the fact that many large Antarctic warming events show a similar fast dust response, with drops of 50 % or more of the initial level within a few centuries (vertical arrows in Fig. 4). There is no obvious threshold in temperature or sea-level that would provoke such fast changes in dust mobilization, especially since dust changes always lead changes in temperature. It would therefore appear that Southern Hemisphere atmospheric changes preceded the main rise of temperature in the Southern Ocean during terminations and Antarctic warming events.

3.2.3 Glacial/interglacial changes in dust distributions

We investigated the distribution of the dust flux during selected 5 kyr time periods. For the Holocene very little LPD data exist (Fig. 1). Moreover, the CPH LPD data over the last 42 kyr were rescaled to the Bern LPD data, and hence do not allow for an independent estimate of the dust flux distribution. Accordingly, we only discussed the $nssCa^{2+}$ distributions over the entire 800 000 year record using 25 year averages of the logarithmised and detrended $nssCa^{2+}$ data. Note however that the overall glacial/interglacial change in the variability of the data discussed below is also seen in the LPD data as illustrated in Fig. 1. The distributions were separately plotted for the interglacials (Fig. 6a) and the glacials (Fig. 6b).

In all studied sections, the distributions of the logarithmic $nssCa^{2+}$ fluxes are well fitted by a unimodal Gaussian distribution with its mean shifted to higher values in glacial

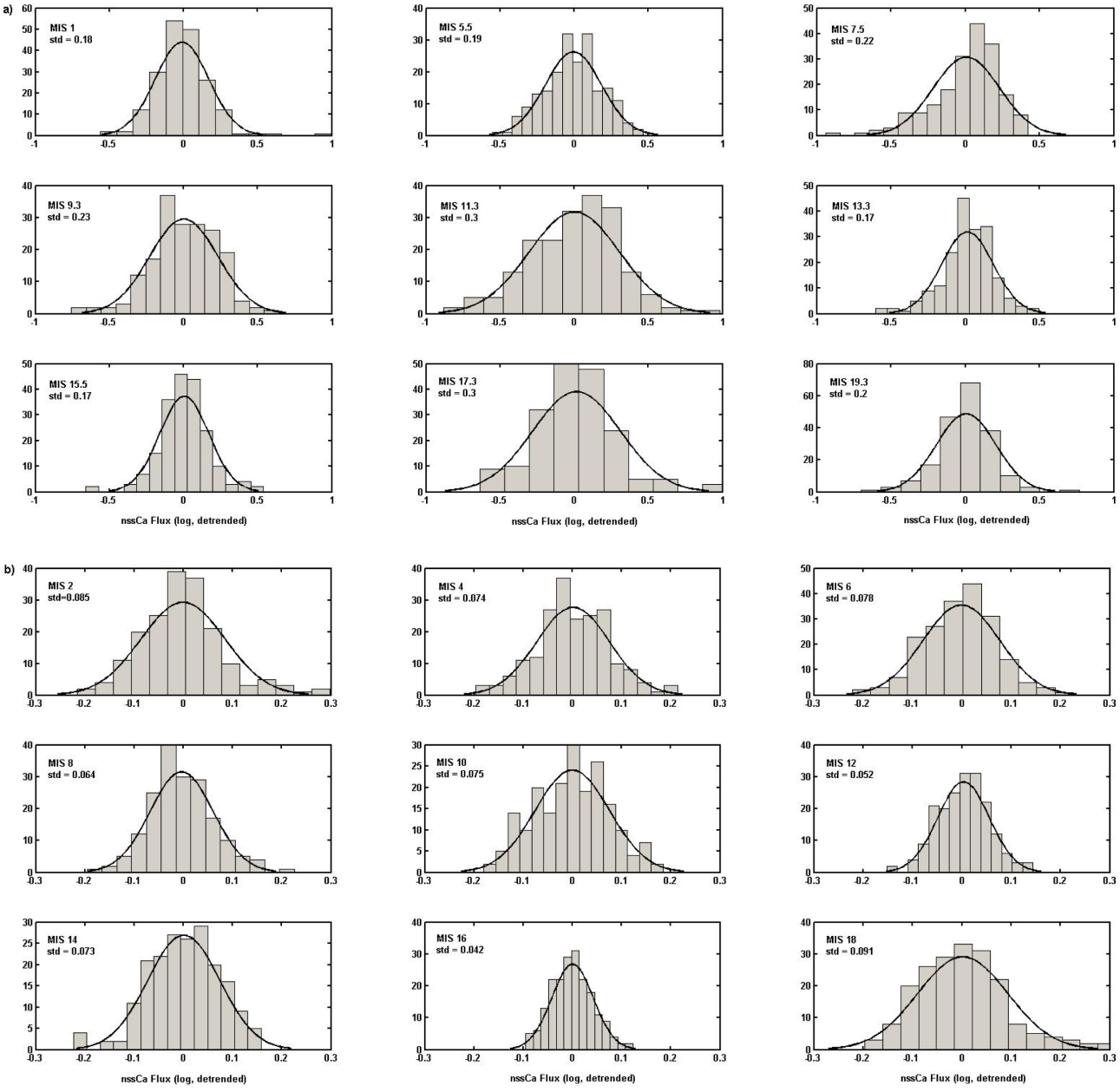

Fig. 6. Distribution during 5 kyr sections of **(a)** interglacials and **(b)** glacials using detrended and logarithmised 25 year mean nssCa^{2+} data. The standard deviations shown are derived from the Gaussian fit.

conditions. This indicates that dust mobilization, transport to, or deposition (or any combination of the three) in Antarctica during glacials were acting on a stronger level than for modern conditions, but that the key processes behind them were never fundamentally different. In particular, extraordinary dust storm events that cannot be described by the background distribution did not occur during glacials, and are therefore not responsible for the very high glacial fluxes. However, there is a distinct difference in the width of the distributions between climatic optima and glacial maxima. Warm periods are characterized by a broad distribution, while cold periods have a markedly narrower one, indicating a higher dust variability around the mean level for warm climate conditions, confirming findings by Bigler et al. (2010). MIS 16, which is thought to have been one of the coldest glacials in the past million years (Lisiecki and Raymo, 2005), shows the narrowest of all distributions, whereas the highest variability is featured during MIS 11, which was the longest interglacial.

The narrower glacial distribution agrees favourably with higher, but steadier wind speed in South America when compared to interglacials. Once again, we can link this to a

latitudinal shift or extension of the westerly wind belt in South America. As has been proposed in Sect. 3.2.2, during cold times, intensive and steadier westerly winds are found in southern South America. This results in a higher and more regular dust mobilization. Vice versa, a stronger sporadic cyclonic activity in this region could explain the higher dust variability for warmer climate conditions. In conjunction with a longer glacial atmospheric residence time due to a weaker hydrological cycle, these changes could explain a large part of the factor of 25 change between glacial and interglacial dust flux (Lambert et al., 2008).

4 Conclusions

The Ca^{2+}, $nssCa^{2+}$ and insoluble particulate dust data from the EPICA Dome C ice core are presented at 1 cm depth resolution, corresponding to a formal sub-annual time resolution at the top and ∼25 years at the bottom of the core.

The calcium to insoluble dust ratio varies by up to a factor of 6 between glacials and interglacials, with higher values during interglacials. These variations could be a result of the additional soluble Ca^{2+} leached by the more acidic atmosphere during warm times and/or of different Ca^{2+} to insoluble dust ratios of the dust sources during both time intervals. Lower $nssCa^{2+}$/dust ratios during early glacial times reflect the earlier increase in sea salt aerosol concentrations at that time.

Using the Ca^{2+}, $nssCa^{2+}$ and insoluble dust records, a new dust flux dataset was created using principal component analysis. The new record reflects the variability common to all three datasets and represents the best high-resolution estimate for atmospheric dust flux variability during the past 800 kyr. Based on this dust flux record, the occurrence of Antarctic warming events was investigated and the events identified during the past eight glacial periods. Such dust imprints of Antarctic warming events can be found during all glacial periods. They occurred about 2–3 times every 10 kyr throughout the last 800 000 years. Southern Hemisphere millennial and centennial variability thus appears to have been a persistent feature of past glacial periods, and points to a similar frequency of rapid changes in the North Atlantic Deep Water formation in the north.

The timing and leads and lags of dust with temperature and CO_2 during glacial terminations were investigated. Dust usually reaches interglacial levels about 4 kyr before both temperature and CO_2. At that time CO_2 levels had never risen by more than 30 ppmv during the last 9 terminations. In addition, the fast reductions in dust flux observed during glacial terminations show no immediate effect on CO_2 concentrations. Iron fertilization by aerosol dust to the Southern Ocean can therefore only explain the smaller part of glacial-interglacial CO_2 changes. The abrupt changes seen in dust flux during terminations and Antarctic warming events within a few centuries suggest that changes in the wind field and in the hydrological cycle in the source region, possibly linked to changes in the latitudinal extension of the Westerlies, may have provoked the sudden drops in dust production and transport. Although not quite as rapid as the decadal atmospheric response to Dansgaard-Oeschger events in the North Atlantic (NGRIP community members, 2004; Steffensen et al., 2008), the centennial jumps in dust flux in central Antarctica indicate quite drastic reconfigurations in the wind regime also in the Southern Hemisphere, linked to climatic changes during the transitions, and leading to substantial dust mobilization changes at that time. Their clear lead on temperature changes suggests that atmospheric reorganization in the Southern Hemisphere occurred before the Southern Ocean had warmed up significantly.

Both glacial and interglacial dust distribution are unimodal and can be well described by a log-normal distribution. Glacials display a narrower standard deviation than interglacials, which we interpret as reflecting the steadier atmospheric conditions in South America during glacial times. We conclude that the processes responsible for dust uptake and transport were not significantly altered from glacial to interglacial conditions. However, replenishment of dust supply, e.g. by glacial outwash, in parallel with higher mean wind speeds, reduced precipitation, and vegetation can explain a largely increased glacial source strength in southern South America. Together with the larger atmospheric residence time connected to lower precipitation en route, this may explain a large part of the 25 times higher dust fluxes in Antarctica during glacials.

Acknowledgements. This work is a contribution to the European Project for Ice Coring in Antarctica (EPICA), a joint European Science Foundation/European Commission scientific programme, funded by the EU and by national contributions from Belgium, Denmark, France, Germany, Italy, the Netherlands, Norway, Sweden, Switzerland and the UK. The main logistic support was provided by IPEV and PNRA (at Dome C) and AWI (at Dronning Maud Land). We thank all the persons involved in the fieldwork to obtain the comprehensive dataset. This is EPICA publication no. 283. Fabrice Lambert is supported by KORDI (PE98801).

Edited by: D.-D. Rousseau

References

Abdi, H. and Williams, L. J.: Principal component analysis, Wiley Interdisciplinary Reviews: Computational Statistics, 2, 433–459, doi:10.1002/wics.101, 2010.

Barker, S., Knorr, G., Edwards, R. L., Parrenin, F., Putnam, A. E., Skinner, L. C., Wolff, E., and Ziegler, M.: 800,000 Years of Abrupt Climate Variability, Science, 347, 0–5, doi:10.1126/science.1203580, 2011.

Bigler, M.: Hochaufloesende Spurenstoffmessungen an polaren Eisbohrkernen: Glazio-chemische und klimatische Prozessstudien, Ph.D. thesis, University of Bern, University of Bern, 2004.

Bigler, M., Röthlisberger, R., Lambert, F., Stocker, T. F., and Wagenbach, D.: Aerosol deposited in East Antarctica over the last glacial cycle: Detailed apportionment of continental and sea-salt contributions, J. Geophys. Res., 111, 1–14, doi:10.1029/2005JD006469, 2006.

Bigler, M., Röthlisberger, R., Lambert, F., Wolff, E. W., Castellano, E., Udisti, R., Stocker, T. F., and Fischer, H.: Atmospheric decadal variability from high-resolution Dome C ice core records of aerosol constituents beyond the Last Interglacial, Quaternary Sci. Rev., 29, 324–337, doi:10.1016/j.quascirev.2009.09.009, 2010.

Blunier, T. and Brook, E. J.: Timing of millennial-scale climate change in Antarctica and Greenland during the last glacial period, Science, 291, 109–112, doi:10.1126/science.291.5501.109, 2001.

Bopp, L.: Dust impact on marine biota and atmospheric CO_2 during glacial periods, Paleoceanography, 18, 1046, doi:10.1029/2002PA000810, 2003.

Bouttes, N., Paillard, D., and Roche, D. M.: Impact of brine-induced stratification on the glacial carbon cycle, Clim. Past, 6, 575–589, doi:10.5194/cp-6-575-2010, 2010.

Bowen, H. J. M.: Environmental Chemistry of the Elements, Academic Press, London, 1979.

Delmonte, B., Petit, J. R., and Maggi, V.: Glacial to Holocene implications of the new 27000-year dust record from the EPICA Dome C (East Antarctica) ice core, Clim. Dynam., 18, 647–660, doi:10.1007/s00382-001-0193-9, 2002.

Delmonte, B., Basile-Doelsch, I., Petit, J.-R., Maggi, V., Revel-Rolland, M., Michard, A., Jagoutz, E., and Grousset, F.: Comparing the Epica and Vostok dust records during the last 220,000 years: stratigraphical correlation and provenance in glacial periods, Earth-Sci. Rev., 66, 63–87, doi:10.1016/j.earscirev.2003.10.004, 2004.

Delmonte, B., Andersson, P. S., Hansson, M., Schöberg, H., Petit, J. R., Basile-Doelsch, I., and Maggi, V.: Aeolian dust in East Antarctica (EPICA-Dome C and Vostok): Provenance during glacial ages over the last 800 kyr, Geophys. Res. Lett., 35, 2–7, doi:10.1029/2008GL033382, 2008.

Delmonte, B., Andersson, P. S., Schöberg, H., Hansson, M., Petit, J. R., Delmas, R., Gaiero, D. M., Maggi, V., and Frezzotti, M.: Geographic provenance of aeolian dust in East Antarctica during Pleistocene glaciations: preliminary results from Talos Dome and comparison with East Antarctic and new Andean ice core data, Quaternary Sci. Rev., 29, 256–264, doi:10.1016/j.quascirev.2009.05.010, 2010.

EPICA community members: One-to-one coupling of glacial climate variability in Greenland and Antarctica, Nature, 444, 195–198, doi:10.1038/nature05301, 2006.

Fischer, H., Fundel, F., Ruth, U., Twarloh, B., Wegner, A., Udisti, R., Becagli, S., Castellano, E., Morganti, A., and Severi, M.: Reconstruction of millennial changes in dust emission, transport and regional sea ice coverage using the deep EPICA ice cores from the Atlantic and Indian Ocean sector of Antarctica, Earth Planet. Sc. Lett., 260, 340–354, doi:10.1016/j.epsl.2007.06.014, 2007a.

Fischer, H., Siggaard-Andersen, M. L., Ruth, U., Röthlisberger, R., and Wolff, E. W.: Glacial/Interglacial changes in mineral dust and sea-salt records in polar ice cores: sources, transport, and deposition, Rev. Geophys., 45, RG1002, doi:10.1029/2005RG000192, 2007b.

Fischer, H., Schmitt, J., Lüthi, D., Stocker, T. F., Tschumi, T., Parekh, P., Joos, F., Köhler, P., Völker, C., Gersonde, R., Barbante, C., Le Floch, M., Raynaud, D., Wolff, E.: The role of Southern Ocean processes in orbital and millennial CO_2 variations – A synthesis, Quaternary Sci. Rev., 29, 193–205, doi:10.1016/j.quascirev.2009.06.007, 2010.

Fuhrer, K., Wolff, E. W., and Johnsen, S. J.: Timescales for dust variability in the Greenland Ice Core Project(GRIP) ice core in the last 100,000 years, J. Geophys. Res., 104, 31043–31052, doi:10.1029/1999JD900929, 1999.

Gaiero, D. M.: Dust provenance in Antarctic ice during glacial periods: From where in southern South America?, Geophys. Res. Lett., 34, 1–6, doi:10.1029/2007GL030520, 2007.

Jouzel, J., Masson-Delmotte, V., Cattani, O., Dreyfus, G., Falourd, S., Hoffmann, G., Minster, B., Nouet, J., Barnola, J. M., Chappellaz, J., Fischer, H., Gallet, J. C., Johnsen, S., Leuenberger, M., Loulergue, L., Luethi, D., Oerter, H., Parrenin, F., Raisbeck, G., Raynaud, D., Schilt, A., Schwander, J., Selmo, E., Souchez, R., Spahni, R., Stauffer, B., Steffensen, J. P., Stenni, B., Stocker, T. F., Tison, J. L., Werner, M., and Wolff, E. W.: Orbital and millennial Antarctic climate variability over the past 800,000 years, Science, 317, 793–796, doi:10.1126/science.1141038, 2007.

Köhler, P. and Fischer, H.: Simulating low frequency changes in atmospheric CO_2 during the last 740 000 years, Clim. Past, 2, 57–78, doi:10.5194/cp-2-57-2006, 2006.

Lässig, J. L., Cogliati, M. G., Bastanski, M. A., and Palese, C.: Wind characteristics in Neuquen , North Patagonia , Argentina, J. Wind Eng. Ind. Aerodyn., 79, 183–199, doi:10.1016/S0167-6105(98)00110-X, 1999.

Lambert, F., Delmonte, B., Petit, J. R., Bigler, M., Kaufmann, P. R., Hutterli, M. A., Stocker, T. F., Ruth, U., Steffensen, J. P., and Maggi, V.: Dust-climate couplings over the past 800,000 years from the EPICA Dome C ice core, Nature, 452, 616–619, doi:10.1038/nature06763, 2008.

Lamy, F., Kilian, R., Arz, H. W., Francois, J.-P., Kaiser, J., Prange, M., and Steinke, T.: Holocene changes in the position and intensity of the southern westerly wind belt, Nat. Geosci., 3, 695–699, doi:10.1038/ngeo959, 2010.

Legrand, M. and Mayewski, P.: Glaciochemistry of polar ice cores: A review, Rev. Geophys., 35, 219–243, doi:10.1029/96RG03527, 1997.

Lisiecki, L. E. and Raymo, M. E.: A Pliocene-Pleistocene stack of 57 globally distributed benthic $\delta^{18}O$ records, Paleoceanography, 20, 1–17, doi:10.1029/2004PA001071, 2005.

Loulergue, L., Schilt, A., Spahni, R., Masson-Delmotte, V., Blunier, T., Lemieux, B., Barnola, J.-M., Raynaud, D., Stocker, T. F., and Chappellaz, J.: Orbital and millennial-scale features of atmospheric CH_4 over the past 800,000 years, Nature, 453, 383–386, doi:10.1038/nature06950, 2008.

Lüthi, D., Le Floch, M., Bereiter, B., Blunier, T., Barnola, J.-M., Siegenthaler, U., Raynaud, D., Jouzel, J., Fischer, H., Kawamura, K., and Stocker, T. F.: High-resolution carbon dioxide concentration record 650,000–800,000 years before present, Nature, 453, 379–382, doi:10.1038/nature06949, 2008.

Maher, B. A., Prospero, J. M., Mackie, D., Gaiero, D., Hesse, P. P., and Balkanski, Y.: Global connections between aeolian dust, climate and ocean biogeochemistry at the present day and at the last glacial maximum, Earth-Sci. Rev., 99, 61–97,

doi:10.1016/j.earscirev.2009.12.001, 2010.

Mahowald, N. M., Muhs, D. R., Levis, S., Rasch, P. J., Yoshioka, M., Zender, C. S., and Luo, C.: Change in atmospheric mineral aerosols in response to climate: Last glacial period, preindustrial, modern, and doubled carbon dioxide climates, J. Geophys. Res., 111, D10202, doi:10.1029/2005JD006653, 2006a.

Mahowald, N. M., Yoshioka, M., Collins, W. D., Conley, A. J., Fillmore, D. W., and Coleman, D. B.: Climate response and radiative forcing from mineral aerosols during the last glacial maximum, pre-industrial, current and doubled-carbon dioxide climates, Geophys. Res. Lett., 33, 2–5, doi:10.1029/2006GL026126, 2006b.

Martin, J. H., Gordon, R. M., and Fitzwater, S. E.: Iron in Antarctic waters, Nature, 345, 156–158, doi:10.1038/345156a0, 1990.

Martin, J. H., Gordon, R. M., and Fitzwater, S. E.: The Case for Iron, Limnol. Oceanogr., 36, 1793–1802, 1991.

Martínez-Garcia, A., Rosell-Melé, A., Geibert, W., Gersonde, R., Masqué, P., Gaspari, V., and Barbante, C.: Links between iron supply, marine productivity, sea surface temperature, and CO_2 over the last 1.1 Ma, Paleoceanography, 24, 1–14, doi:10.1029/2008PA001657, 2009.

Martínez-Garcia, A., Rosell-Melé, A., Jaccard, S. L., Geibert, W., Sigman, D. M., and Haug, G. H.: Southern Ocean dust – climate coupling over the past four million years, Nature, 476, 312–315, doi:10.1038/nature10310, 2011.

Martrat, B., Grimalt, J. O., Shackleton, N. J., de Abreu, L., Hutterli, M. A., and Stocker, T. F.: Four climate cycles of recurring deep and surface water destabilizations on the Iberian margin., Science (New York, N.Y.), 317, 502–507, doi:10.1126/science.1139994, 2007.

Mayewski, P. A., Meeker, L. D., Whitlow, S., Twickler, M. S., Morrison, M. C., Bloomfield, P., Bond, G. C., Alley, R. B., Gow, A. J., Meese, D. A., Grootes, P. M., Ram, M., Taylor, K. C., and Wumkes, W.: Changes in Atmospheric Circulation and Ocean Ice Cover over the North Atlantic During the Last 41,000 Years, Science, 263, 1747–1751, doi:10.1126/science.263.5154.1747, 1994.

Miller, R. L. and Tegen, I.: Climate Response to Soil Dust Aerosols, J. Climate, 11, 3247–3267, doi:10.1175/1520-0442(1998)011<3247:CRTSDA>2.0.CO;2, 1998.

NGRIP community members: High-resolution record of Northern Hemisphere climate extending into the last interglacial period, Nature, 431, 147–151, doi:10.1038/nature02805, 2004.

Rankin, A. M., Auld, V., and Wolff, E. W.: Frost flowers as a source of fractionated sea salt aerosol in the polar regions, Geophys. Res. Lett., 27, 3469, doi:10.1029/2000GL011771, 2000.

Revel-Rolland, M., Dedeckker, P., Delmonte, B., Hesse, P., Magee, J., Basiledoelsch, I., Grousset, F., and Bosch, D.: Eastern Australia: A possible source of dust in East Antarctica interglacial ice, Earth Planet. Sc. Lett., 249, 1–13, doi:10.1016/j.epsl.2006.06.028, 2006.

Ridgwell, A. J.: Implications of the glacial CO_2 "iron hypothesis" for Quaternary climate change, Geochem. Geophy. Geosy., 4, 1–10, doi:10.1029/2003GC000563, 2003.

Röthlisberger, R., Bigler, M., Hutterli, M., Sommer, S., Stauffer, B., Junghans, H. G., and Wagenbach, D.: Technique for continuous high-resolution analysis of trace substances in firn and ice cores, Environ. Sci. Technol, 34, 338–342, doi:10.1021/es9907055, 2000.

Röthlisberger, R., Mulvaney, R., Wolff, E. W., Hutterli, M. A., Bigler, M., Sommer, S., and Jouzel, J.: Dust and sea salt variability in central East Antarctica (Dome C) over the last 45 kyrs and its implications for southern high-latitude climate, Geophys. Res. Lett., 29, 1-5, doi:10.1029/2002GL015186, 2002.

Röthlisberger, R., Bigler, M., Wolff, E. W., Joos, F., Monnin, E., and Hutterli, M. A.: Ice core evidence for the extent of past atmospheric CO_2 change due to iron fertilisation, Geophys. Res. Lett., 31, 2–5, doi:10.1029/2004GL020338, 2004.

Ruth, U., Wagenbach, D., Bigler, M., Steffensen, J. P., Röthlisberger, R., and Miller, H.: High resolution microparticle profiles at NGRIP: case studies of the calcium-dust relationship, Ann. Glaciol., 35, 237–242, 2002.

Ruth, U., Wagenbach, D., Steffensen, J. P., and Bigler, M.: Continuous record of microparticle concentration and size distribution in the central Greenland NGRIP ice core during the last glacial period, J. Geophys. Res., 108, 1–12, doi:10.1029/2002JD002376, 2003.

Ruth, U., Barbante, C., Bigler, M., Delmonte, B., Fischer, H., Gabrielli, P., Gaspari, V., Kaufmann, P., Lambert, F., Maggi, V., Marino, F., Petit, J.-R., Udisti, R., Wagenbach, D., Wegner, A., and Wolff, E. W: Proxies and measurement techniques for mineral dust in Antarctic ice cores, Environ. Sci. Technol., 42, 5675–5681, doi:10.1021/es703078z, 2008.

Sassen, K., Demott, P. J., Prospero, J. M., and Poellot, M. R.: Saharan dust storms and indirect aerosol effects on clouds?: CRYSTAL-FACE results, Geophys. Res. Lett., 30, 1–4, doi:10.1029/2003GL017371, 2003.

Schwartz, S. E.: The whitehouse effect-shortwave radiative forcing of climate by anthropogenic aerosols: an overview, J. Aerosol. Sci., 27, 359–382, doi:10.1016/0021-8502(95)00533-1, 1996.

Sigman, D. M., Hain, M. P., and Haug, G. H.: The polar ocean and glacial cycles in atmospheric CO(2) concentration, Nature, 466, 47–55, doi:10.1038/nature09149, 2010.

Steffensen, J. P., Andersen, K. K., Bigler, M., Clausen, H. B., Dahl-Jensen, D., Fischer, H., Goto-Azuma, K., Hansson, M., Johnsen, S. J., Jouzel, J., Masson-Delmotte, V., Popp, T., Rasmussen, S. O., Röthlisberger, R. R., Stauffer, U., Siggaard-Andersen, B., Sveinbjörnsdóttir, M. L., Arny, E., Svensson, A., and White, J. W. C.: High-resolution Greenland ice core data show abrupt climate change happens in few years, Science, 321, 680–684, doi:10.1126/science.1157707, 2008.

Stocker, T. F. and Johnsen, S. J.: A minimum thermodynamic model for the bipolar seesaw, Paleoceanography, 18, 1087–1089, doi:10.1029/2003PA000920, 2003.

Sugden, D. E., McCulloch, R. D., Bory, A. J.-M., and Hein, A. S.: Influence of Patagonian glaciers on Antarctic dust deposition during the last glacial period, Nat. Geosci., 2, 281–285, doi:10.1038/ngeo474, 2009.

Tegen, I.: Modeling the mineral dust aerosol cycle in the climate system, Quaternary Sci. Rev., 22, 1821–1834, doi:10.1016/S0277-3791(03)00163-X, 2003.

Tegen, I., Lacis, A., and Fung, I.: The influence on climate forcing of mineral aerosols from disturbed soils, Nature, 380, 419–422, doi:10.1038/380419a0, 1996.

Watson, A. J., Bakker, D. C., Ridgwell, A. J., Boyd, P. W., and Law, C. S.: Effect of iron supply on Southern Ocean CO_2 uptake and implications for glacial atmospheric CO_2, Nature, 407, 730–733, doi:10.1038/35037561, 2000.

Winckler, G. and Fischer, H.: 30,000 years of cosmic dust in Antarctic ice, Science, 313, 491, doi:10.1126/science.1127469, 2006.

Wolff, E. W., Fischer, H., Fundel, F., Ruth, U., Twarloh, B., Littot, G. C., Mulvaney, R., Röthlisberger, R., de Angelis, M., Boutron, C. F., Hansson, M., Jonsell, U., Hutterli, M. A., Lambert, F., Kaufmann, P., Stauffer, B., Stocker, T. F., Steffensen, J. P., Bigler, M., Siggaard-Andersen, M. L., Udisti, R., Becagli, S., Castellano, E., Severi, M., Wagenbach, D., Barbante, C., Gabrielli, P., and Gaspari, V.: Southern Ocean sea-ice extent, productivity and iron flux over the past eight glacial cycles, Nature, 440, 491–496, doi:10.1038/nature04614, 2006.

Wolff, E., Fischer, H., and Röthlisberger, R.: Glacial terminations as southern warmings without northern control, Nat. Geosci., 2, 206–209, doi:10.1038/NGEO442, 2009.